Controlled Doping in Thin-Film Transistors of Large Contorted Aromatic Compounds**

Shengxiong Xiao, Seok Ju Kang, Yu Zhong, Shengguo Zhang, Amy M. Scott, Alberto Moscatelli, Nicholas J. Turro, Michael L. Steigerwald, Hexing Li,* and Colin Nuckolls*
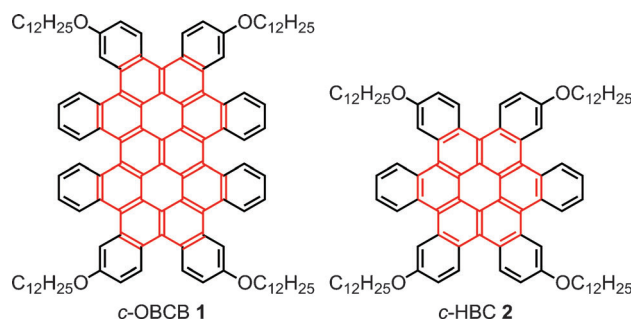
Dedicated to Sandra Turro

Herein, we describe a new thin-film organic material that forms the active layer in an organic field-effect transistor (OFET)[1–6] and can be switched simultaneously by using two different inputs, that is, electrical bias and protonation. The thin materials are formed from a new contorted aromatic compound (c-OBCB **1**) that has an expanded central core (Scheme 1). This polycyclic aromatic hydrocarbon (PAH) can be protonated by exposure to acid and the resulting cations are stable under ambient conditions. In thin-film transistors,

Scheme 1. Dodecyloxy-substituted contorted aromatic compounds, ring-expanded octabenzocircumbiphenyl (c-OBCB **1**) and hexabenzo-coronene (c-HBC **2**).

[*] Dr. S. Xiao, Prof. H. Li, Prof. C. Nuckolls
Department of Chemistry
Optoelectronic Nano Materials and Devices Institute
Shanghai Normal University, Shanghai (China)
E-mail: hexing-Li@shnu.edu.cn

Dr. S. Xiao, Dr. S. J. Kang, Y. Zhong, S. Zhang, Dr. A. M. Scott,
Dr. A. Moscatelli, Prof. N. J. Turro, Dr. M. L. Steigerwald,
Prof. C. Nuckolls
Department of Chemistry
Columbia University, New York, NY 10027 (USA)
E-mail: cn37@columbia.edu

the PAH−H$^+$ formed acts as a chemical oxidant that positions carriers at the interface of the dielectric layer by a series of electron transfers. In the protonated films with no applied gate bias, the device is in the on state, and the carriers can be depleted from the channel by applying an electrical gate bias to switch the transistor to the off state. In this way the two inputs, protonation and electrical bias, can work synergist-ically in this new type of multimode transistor. The effect is reversible, and removing the dopants (i.e., protons) restores the transistors to a typical OFET operation where the carriers are accumulated in the channel with a gate bias. The advantage of molecular-based electronic materials is that they can be tailored by chemical synthesis to have functions beyond simply carrying current.[7–15] This approach provides new information processing strategies with the capacity to switch,[16] actuate, and sense to modulate conductivity[10,12,13,16] and a design strategy for organic switches[17,18] employing chemical inputs.

The dodecyloxy-substituted contorted octabenzocircum-biphenyl (c-OBCB; **1**; Scheme 1) is a ring-expanded version of a class of electronic materials formed from contorted aromatics known as contorted hexabenzocoronene (c-HBC; **2**).[9] Typical derivatives of c-HBC form hole-transporting semiconducting thin films and have shown field-effect hole mobility as high as 1 cm^2 V^{-1} s.[10,11] The c-OBCB skeleton can be protonated when exposed to acid, and the resulting conjugate acids are persistent; they do not degrade or undergo subsequent irreversible rearrangements.

The design of the ring-expanded c-OBCB **1** was based on that of c-HBC (**2**), which when substituted with four dodecyloxy groups forms a columnar liquid crystalline phase where the columns align parallel to the substrate.[9] To synthesize the extremely crowded tris-olefin **5**, we use a Barton–Kellogg olefination,[19–21] which joins the two pentacene fragments **3** and **4** (Scheme 2). We cyclize **5** by using a Katz-modified Mallory photocyclization[22,23] to yield **1** (see the Supporting Information for full details of the synthesis and characterization).

c-OBCB **1** forms a rectangular arrangement of molecular columns, as seen in the powder X-ray diffractogram (see the Supporting Information, Figure S1). In a related study, we have shown that films of the c-OBCB act as the *p*-type organic semiconductor in an OFET, and they can serve as a donor material in an organic photovoltaic device when mixed with fullerenes. The HOMO (−5.4 ev) and LUMO (−3.0 eV) were measured by using cyclic voltammetry with a ferrocene standard.[24]
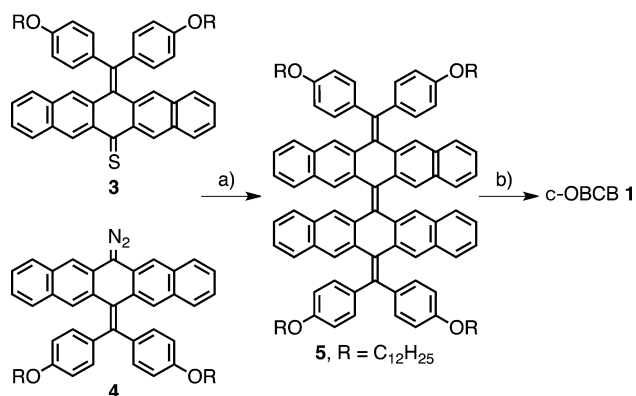
Scheme 2. Synthesis of the dodecyloxy-substituted c-OBCB **1**. Reaction conditions: a) PPh$_3$; b) $h\nu$, I$_2$, propylene oxide, anhydrous benzene.

The property that we exploit here is the well-known ability of coronenes to act as Brønsted bases.[25–30] Our hypothesis is that c-OBCB would be more easily protonated because it has an expanded core, and would produce a more stable, delocalized cation than its smaller aromatic analogues. Figure 1 and Figure S2 (see the Supporting Information) show the UV/Vis spectra of solutions (dichloromethane) and films c-OBCB treated with triflic acid (CF$_3$SO$_3$H). Upon treatment with acid, the solutions change color from yellow to deep blue. After exposure to triflic acid, long-wavelength absorbance is seen in the UV/Vis spectra of both the solution in dichloromethane and the film (25 nm thick; Figure 1 and Figure S2B in the Supporting Information). This absorption is similar to that seen for the aromatic radical cation of dicoronylene.[31] We see similar long-wavelength features when trifluoroacetic acid (Figure S2A in the Supporting Information) or HBr gas are used in solution. We did not detect these long-wavelength absorbances in films that were

Figure 1. A) Comparison of the UV/Vis spectra of c-OBCB **1** in solution (1×10^{-5} M in CH$_2$Cl$_2$, 1 cm path length) before (red curve) and after (green curve) addition of triflic acid (15 μL to 3 mL of solution). B) UV/Vis of a thin film of c-OBCB **1** on quartz before (red curve) and after (green curve) exposure to triflic acid vapor.

exposed to trifluoroacetic acid (Figure S2C in the Supporting Information), but we detected the protonation through OFET measurements described below.

The films and solutions containing these cations are stable in an ambient atmosphere. We have not been able to obtain a crystal structure to determine the site or sites of protonation on the c-OBCB. We speculate that the protonation sites are in the core of the c-OBCB (the red region of **1** in Scheme 1) because the exterior phenyl groups provide an insulating sheath around the outside of the molecule.[32] The band at 550 nm in the spectrum of the unprotonated solution and that of the film of **1** is attributed to the absorbance of the triplet band in UV/Vis.[32] It is difficult to assign this band in the protonated spectra owing to the multitude of long-wavelength absorbances.
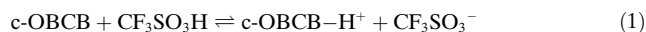
In the films exposed to triflic acid, the long-wavelength absorbance (ca. 700 nm, marked cation in Figure 1B) characteristic of the cation, c-OBCB−H$^+$, is clearly present. The change in intensity of this absorption with exposure over time is shown in Figure S2C (see the Supporting Information). The band at approximately 500 nm, which is indicative of the unprotonated c-OBCB, is still present, thus implying that only a fraction of the material is protonated in the films. By exposing the films to triflic acid at higher temperatures, we confirmed that only a fraction of the material is protonated; the spectra of the resulting films contained a more intense band corresponding to the cation (Figure S2C in the Supporting Information). The films do not have sufficient porosity to allow penetration of the proton and the corresponding counterions into the bulk of the film. When we neutralize solutions of the protonated compound the long-wavelength absorbance disappears, and the original spectrum of the unprotonated c-OBCB is recovered. When the acid-treated films are placed in a vacuum, the long-wavelength absorbance disappears as the acid is removed, thus indicating that the protonation is reversible and does not chemically degrade the sample. We were able to repeat this at least ten times.

When protonated through intermolecular electron transfer, coronene and other aromatic compounds form radicals that can serve as one-electron oxidants in both solution and the solid state.[25–27,33,34] To confirm the presence of the radical cation, c-OBCB$^{+\bullet}$, the EPR spectrum of c-OBCB **1** was recorded, in the absence of oxygen, both in dichloromethane and in the solid state, before and after exposure to triflic acid. The steady-state spectrum is shown in Figure S3 (see the Supporting Information), and in both protonated cases a strong, featureless resonance at ca. 3480 G is observed that is typical of carbon-centered radicals. We do not observe any hyperfine coupling in these spectra at room temperature under these conditions; however, the resolution of the EPR spectrum and the intensity of hyperfine couplings are sensitive to the environment and influenced by sample concentration, temperature, and the physical properties of the solvent, therefore varying these parameters empirically may result in a more resolved EPR profile.[25–27,33,34] Treatment of c-OBCB **1** with either triflic acid or trifluoroacetic acid results in qualitatively similar EPR spectra, however, the magnitude of the EPR signal is greater in the triflic acid case (when equivalent molar amounts of the acids were used).
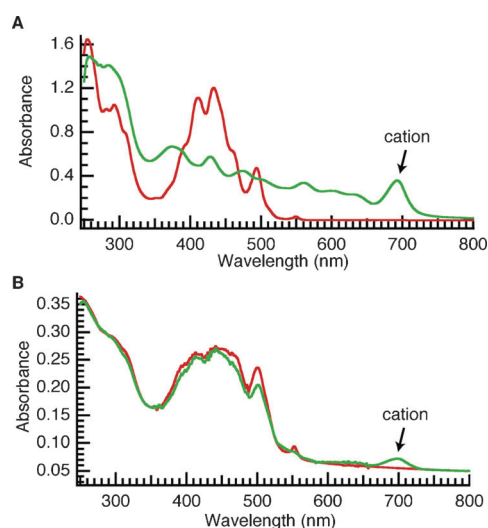
Triflic acid itself is not an oxidant, but in the presence of an oxidizing agent, or in the presence of UV radiation and oxygen, the radical cations of dibenzo-p-dioxins have been observed.[34] In this case and in several other examples, in the absence of oxygen the radical cation still persists.[33] The mechanism for oxidation in the presence of triflic acid as a Brønsted acid, to form c-OBCB−H$^{+\cdot}$ is shown by the following equations:

$$c\text{-OBCB} + CF_3SO_3H \rightleftharpoons c\text{-OBCB}-H^+ + CF_3SO_3^- \qquad (1)$$

$$c\text{-OBCB}-H^+ + c\text{-OBCB} \rightleftharpoons c\text{-OBCB}-H^\cdot + c\text{-OBCB}^{+\cdot} \qquad (2)$$

To determine how the layer of protonated PAH in the thin film influences electrical properties, we fabricated OFETs with c-OBCB **1** and then subjected the devices to acid vapor (Figure 2 A). Before it is exposed to acid, the device exhibits characteristics of a typical OFET (Figure 2 B and C). The c-OBCB is a *p*-type, hole-transporting semiconductor. The mobility, threshold voltage, and on/off ratio for this device are 2.4×10^{-3} cm^{2}V^{-1}s^{-1}, −5.0 V, and 6.7×10^3, respectively. The mobility is calculated by plotting $|I_{DS}|^{1/2}$ versus $|V_G|$ and using the equation: $I_{DS} = (\mu W C_i/2L)(V_G-V_0)^2$ with W (electrode width) = 2 mm and L (channel length) = 100 μm; the source-drain voltage is fixed at −100 V, in the saturation regime of the current–voltage curves (Figure 2 B).

The electrical characteristics change dramatically when the OFETs made from c-OBCB are exposed to trifluoroacetic acid. This change is shown in Figure 2 D and Figure 2 E. The transistor can now be operated in depletion or "turn-off" mode. It is important to note that at zero gate bias the protonated device already shows essentially the same current level as the unprotonated device at $V_g = 0$ V in Figure 2 B. As a positive gate bias is applied, the holes are depleted and the device can be converted into the off state. The mobility, on/off ratio, and threshold voltage are 7×10^{-4} cm^{2}V^{-1}s^{-1}, 1.5×10^3, and 88 V, respectively. Importantly, the device is in the on state after exposure to trifluoroacetic acid, and the gate electrode can deplete the carriers in the channel. This is opposite from the operation of typical organic field-effect transistors in which carriers are introduced by application of a gate bias voltage. The reversibility with respect to acid treatment and removal, which we observed in the optical behavior of c-OBCB (see above), is observed in the electrical behavior of these devices. After the acid-treated devices are placed in a vacuum for a few hours, the device behaves qualitatively as it did before treatment with acid. The carriers are now no longer in the channel and the device operates as a standard OFET where a bias introduces the carriers. There are some quantitative differences in the absolute current levels and mobility in the devices. This data is shown in Figure S4 in the Supporting Information. We were able to repeat this process four times.

When triflic acid, the stronger acid, is used the device is also very conductive. Figure 3 shows the performance of a device after it has been exposed to triflic acid vapor for 5 min. In the case of triflic acid the device is so heavily doped that it cannot be turned off with a gate bias. The resistance of the treated film is six orders of magnitude lower than that of the untreated film ($V_G = 0$ V). We can also reverse this process by applying a vacuum to the sample.

The origin of the effect of the doping process with acid is twofold. 1) As is shown in Figure 2 A, the layer of protonated material is on the surface of the film and in an OFET configuration with the source and drain electrodes. The originally formed cation, c-OBCB−H$^+$, is not the carrier in the films, as if it were, at minimum, the movement of protons would be required for conduction to occur. The carriers must be the electrons/holes represented by the radical cations[35] and produced through charge transfer as described by equations (1) and (2).[36] The charge transport is then the thermoneutral charge transfer between c-OBCB$^{+\cdot}$ and c-OBCB. As with the cation, the radical is not the carrier because then the movement of a hydrogen atom would be required for conduction to occur. We see evidence in the EPR spectra (Figure S3) in films for the formation of c-OBCB$^{+\cdot}$ upon protonation. 2) Importantly, the counterion, trifluoroacetate, will be localized at the top of the film, thus creating a dipole layer. We do not anticipate that the counterions will be able to penetrate the entire film, based on the UV/Vis data in Figure 1 B, thus creating a dipole field into the channel in the same way that a gate bias introduces
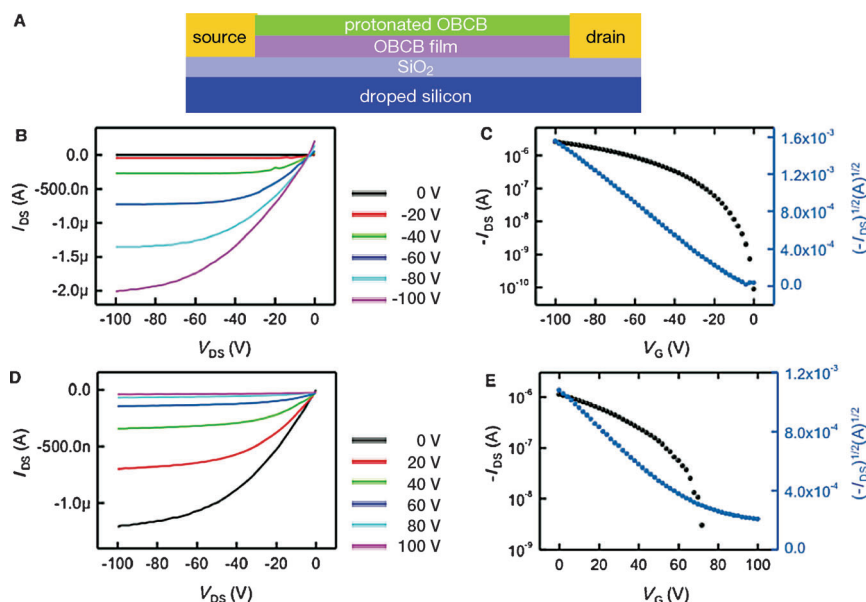
Figure 2. A) Schematic of a thin-film field-effect transistor made from c-OBCB **1** after its exposure to triflic acid. Electrode width $W = 2$ mm and channel length $L = 100$ μm. B) Transistor output before treatment with acid. $V_G = 0$ and −100 V in −20 V steps. C) Transfer characteristics before treatment with acid. $V_{DS} = -100$ V. D) Transistor output after treatment with trifluoroacetic acid. $V_G = 0$ and 100 V in 20 V steps. E) Transfer characteristics after treatment with acid. $V_{DS} = -100$ V.
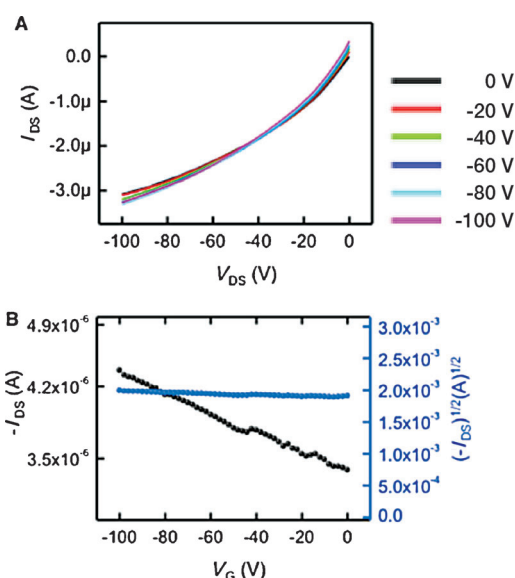
Figure 3. Performance of a thin-film field-effect transistor made from c-OBCB **1** after its exposure to triflic acid. Electrode width $W = 2$ mm and channel length $L = 100$ μm (A) S-D bias at 0 gate voltage after exposure to triflic acid vapor. B) Transfer characteristics after exposure to triflic acid vapor. $V_{DS} = -100$ V.

a field in the channel of a transistor. This field, and the associated electron transfers, position the carriers at the interface with the gate dielectric to turn the device on, thus creating a chemical capacitor on top of the unprotonated material. To test this theory we made OFET devices where we spin cast films from acidic solution. This method should randomly distribute cations and cation radicals in the film but the films will lack the dipole layer. Although the films have spectroscopic signatures of the cations, we see only degraded electrical characteristics.

Herein, we have presented is a new chemical method for controlling the doping levels in organic semiconductor films. In contrast to polymer-based electronics, there are few ways to controllably dope molecular semiconductors. Previously, doping techniques of OFETs were limited to doping of thiophene-based polymer semiconductors, mostly poly(3-hexylthiophene) (P3HT), with electrochemical dopants of such as tetraethylammonium perchlorate,[37,38] 2,3,5,6-tetra-fluoro-7,7,8,8-tetracyanoquinodimethane (F4-TCNQ),[39,40] and 4-ethyl-benzenesulfonic acid (EBSA) acid.[41,42] Doping of pentacene-based OFETs with F4-TCNQ forms a charge transfer complex.[43,44] In each case, the material goes from an off state when undoped to an on state when doped. In each of these cases, however, the materials have not been switchable with a gate field. Our study represents a new method for doping of molecular semiconductors that produces films that can be turned off with an applied gate field.

This study centers on the discovery that Brønsted acids protonate the contorted OBCB and the resulting cations are stable. The protonated PAH, in the absence of oxygen, initiates charge-transfer reactions, resulting in the doping of the semiconducting film. The counterions localized at the surface of the film act as a chemical version of a capacitor to switch the device on. The device can be switched off by applying a gate bias. These studies open the way for the development of other types of multimode switching based on a variety of recognition and binding phenomenon.

[1] K. Takimiya, S. Shinamura, I. Osaka, E. Miyazaki, *Adv. Mater.* **2011**, *23*, 4347–4370.
[2] A. Facchetti, *Chem. Mater.* **2011**, *23*, 733–758.
[3] Y. Liu, Y. Liu, X. Zhan, *Macromol. Chem. Phys.* **2011**, *212*, 428–443.
[4] H. Usta, A. Facchetti, T. Marks, *Acc. Chem. Res.* **2011**, *44*, 501–510.
[5] M. Mas-Torrent, C. Rovira, *Chem. Rev.* **2011**, *111*, 4833–4856.
[6] C.-a. Di, Y. Liu, D. Zhu, *Acc. Chem. Res.* **2009**, *42*, 1573–1583.
[7] A. Operamolla, G. M. Farinola, *Eur. J. Org. Chem.* **2011**, 423–450.
[8] J. Janata, M. Josowicz, *J. Solid State Electrochem.* **2009**, *13*, 41–49.
[9] S. X. Xiao, M. Myers, Q. Miao, S. Sanaur, K. L. Pang, M. L. Steigerwald, C. Nuckolls, *Angew. Chem.* **2005**, *117*, 7556–7560; *Angew. Chem. Int. Ed.* **2005**, *44*, 7390–7394.
[10] X. Guo, M. Myers, S. Xiao, M. Lefenfeld, R. Steiner, G. S. Tulevski, J. Tang, J. Baumert, F. Leibfarth, J. T. Yardley, M. L. Steigerwald, P. Kim, C. Nuckolls, *Proc. Natl. Acad. Sci. USA* **2006**, *103*, 11452–11456.
[11] S. X. Xiao, J. Y. Tang, T. Beetz, X. F. Guo, N. Tremblay, T. Siegrist, Y. M. Zhu, M. Steigerwald, C. Nuckolls, *J. Am. Chem. Soc.* **2006**, *128*, 10700–10701.
[12] X. F. Guo, S. X. Xiao, M. Myers, Q. Miao, M. L. Steigerwald, C. Nuckolls, *Proc. Natl. Acad. Sci. USA* **2009**, *106*, 691–696.
[13] J. Wu, W. Pisula, K. Müllen, *Chem. Rev.* **2007**, *107*, 718–747.
[14] C. Klinke, A. Afzali, P. Avouris, *Chem. Phys. Lett.* **2006**, *430*, 75–79.
[15] J. H. Back, M. Shim, *J. Phys. Chem. B* **2006**, *110*, 23736–23741.
[16] P. Lutsyk, K. Janus, J. Sworakowski, G. Generali, R. Capelli, M. Muccini, *J. Phys. Chem. C* **2011**, *115*, 3106–3114.
[17] S. Huettner, M. Sommer, J. Hodgkiss, P. Kohn, T. Thurn-Albrecht, R. H. Friend, U. Steiner, M. Thelakkat, *ACS Nano* **2011**, *5*, 3506–3515.
[18] W. Takashima, T. Murasaki, S. Nagamatsu, T. Morita, K. Kaneto, *Appl. Phys. Lett.* **2007**, *91*, 071905–071908.
[19] R. M. Kellogg, *Tetrahedron* **1976**, *32*, 2165–2184.
[20] D. H. R. Barton, J. Willis, *J. Chem. Soc. D* **1970**, 1225–1226.
[21] B. L. Feringa, *Acc. Chem. Res.* **2001**, *34*, 504–513.
[22] F. B. Mallory, C. S. Wood, J. T. Gordon, L. C. Lindquist, M. L. Savitz, *J. Am. Chem. Soc.* **1962**, *84*, 4361–4362.
[23] L. Liu, B. Yang, T. Katz, M. K. Poindexter, *J. Org. Chem.* **1991**, *56*, 3769–3775.
[24] S. Xiao, S. J. Kang, Y. Wu, S. Ahn, J. B. Kim, Y.-L. Loo, T. Siegrist, M. L. Steigerwald, H. Li, C. Nuckolls, *Chem. Sci.*, DOI: 10.1039/c3sc50374g.
[25] K. K. Laali, J. J. Houser, M. Zander, *J. Chem. Soc. Perkin Trans. 2* **1996**, 1265–1269.
[26] K. K. Laali, J. J. Houser, *J. Chem. Soc. Perkin Trans. 2* **1994**, 1303–1308.
[27] K. K. Laali, *Chem. Rev.* **1996**, *96*, 1873–1906.
[28] J. R. Bolton, A. Carrington, *Mol. Phys.* **1961**, *4*, 271–272.
[29] H. van Willigen, *J. Chem. Phys.* **1968**, *49*, 1190–1190.

[30] H. Ohya-Nishiguchi, H. Ide, N. Hirota, *Chem. Phys. Lett.* **1979**, *66*, 581 – 583.

[31] F. Cataldo, S. Iglesias-Groth, A. Manchado, *Spectrochim. Acta Part A* **2010**, *77*, 998 – 1004.

[32] Y. S. Cohen, S. Xiao, M. L. Steigerwald, C. Nuckolls, C. R. Kagan, *Nano Lett.* **2006**, *6*, 2838 – 2841.

[33] R. Rathore, C. Zhu, S. V. Lindeman, J. K. Kochi, *J. Chem. Soc. Perkin Trans. 2* **2000**, 1837 – 1840.

[34] G. C. Yang, A. E. Pohland in *Advances in Chemistry* (Ed.: E. Blair), American Chemical Society, Washington, **1973**.

[35] E. de Boer, S. I. Weissman, *J. Am. Chem. Soc.* **1958**, *80*, 4549 – 4555.

[36] S. M. Hubig, S. V. Lindeman, J. K. Kochi, *Coord. Chem. Rev.* **2000**, *200 – 202*, 831 – 873.

[37] X. Jiang, Y. Harima, K. Yamashita, Y. Tada, J. Ohshita, A. Kunai, *Chem. Phys. Lett.* **2002**, *364*, 616 – 620.

[38] V. I. Arkhipov, P. Heremans, E. V. Emelianova, G. J. Adriaenssens, H. Bassler, *Appl. Phys. Lett.* **2003**, *82*, 3245 – 3247.

[39] E. Lim, B. J. Jung, M. Chikamatsu, R. Azumi, Y. Yoshida, K. Yase, L. M. Do, H. K. Shim, *J. Mater. Chem.* **2007**, *17*, 1416 – 1420.

[40] L. Ma, W. H. Lee, Y. D. Park, J. S. Kim, H. S. Lee, K. Choa, *Appl. Phys. Lett.* **2008**, *92*, 063310 – 063313.

[41] S. Nam, J. Kim, H. Lee, H. Kim, C.-S. Ha, Y. Kim, *ACS Appl. Mater. Interfaces* **2012**, *4*, 1281 – 1288.

[42] S. Nam, M. Shin, H. Kim, C.-S. Ha, M. Ree, Y. Kim, *Adv. Funct. Mater.* **2011**, *21*, 4527 – 4534.

[43] Y. Abe, T. Hasegawa, Y. Takahashi, T. Yamada, Y. Tokura, *Appl. Phys. Lett.* **2005**, *87*, 153506.

[44] T. Minari, T. Miyadera, K. Tsukagoshi, Y. Aoyagi, H. Ito, *Appl. Phys. Lett.* **2007**, *91*, 053508.